

Helicity degree of carrageenan conformation determines the 2 polysaccharide and water interactions

by Elmarhoum, S., Ako, K., Munialo, C.D. and Rharbi, Y.

Copyright, publisher and additional information: Publishers' version distributed under the terms of the [Creative Commons Attribution NonCommercial NoDerivatives License](#)

[DOI link to the version of record on the publisher's site](#)



Elmarhoum, S., Ako, K., Munialo, C.D. and Rharbi, Y. 2023. Helicity degree of carrageenan conformation determines the polysaccharide and water interactions. *Carbohydrate Polymers*, 314, article number 120952

15 August 2023

1 Helicity degree of carrageenan conformation determines the 2 polysaccharide and water interactions

3
4 **Authors and affiliations:**

5 Said ELMARHOUM^a, Komla AKO ^{*a}, Claire D. MUNIALO^b & Yahya RHARBI^a

6 a) Univ. Grenoble Alpes, CNRS, Grenoble INP, LRP, 38000 Grenoble, France

7 b) Food Land and Agribusiness Management Department Harper Adams University Newport,
8 Shropshire, TF10 8NB, UK

9 ***Corresponding author:** *komla.ako@univ-grenoble-alpes.fr; akokomla@hotmail.com*

10

11 **Abstract:**

12 The polysaccharide in solution at critical concentration, C_c (g/L), is assimilated to a nano
13 hydrogel (nHG) made of a single polysaccharide chain. Taking as reference the characteristic
14 temperature of 20 ± 2 °C at which kappa-carrageenan (κ -Car) nHG swelling is greater with a
15 $C_c = 0.55 \pm 0.05$ g/L, the temperature of the minimum deswelling in presence of KCl was
16 found at 30 ± 2 °C for 5 mM with a $C_c = 1.15 \pm 0.05$ g/L but not measurable above 100 °C
17 for 10 mM of which $C_c = 1.3 \pm 0.05$ g/L. Lowering the temperature to 5 °C, contraction of the
18 nHG and further coil-helix transition with self-assembly increases the sample's viscosity,
19 which steadily evolves with time in a logarithmic scale. Accordingly, the relative increment of
20 the viscosity per unit of concentration, R_v (L/g), should increase in agreement with increasing
21 polysaccharide concentration. But the R_v decreases for κ -Car samples above 3.5 ± 0.5 g/L in
22 the presence of 10 mM KCl under steady shear 15 s⁻¹. This reflects a decrease of κ -Car
23 helicity degree knowing that the polysaccharide is rather hydrophilic when its helicity degree
24 is the lowest.

25 **Keywords:** Polysaccharide; Nanohydrogel; Kinetic; Coil-helix; Reduced viscosity

26 **1 Introduction**

27 As dissolution of the polysaccharides in aqueous phase precede most of the polysaccharide
28 applications in food and nonfood areas, understanding their solubility, therefore, becomes
29 critically important (Elfaruk, Wen, Chi & Li, 2021; Gerentes, Vachoud, Doury & Domard,
30 2002). For example, pectin, starch, agarose and chitosan powders have to be dissolved in
31 aqueous media prior to any application (Einhorn-Stoll, 2018; Felfel, Gideon-Adeniyi,
32 Hossain, Roberts & Grant, 2019; Saeedi Garakani et al., 2020; Yousefi & Ako, 2020).
33 Solubilization of polysaccharide in water is currently performed at high temperature ($> 60\text{ }^{\circ}\text{C}$)
34 then cooled for applications such as stabilizer in food, scaffold in tissue engineering and
35 matrix in personal care (Fabra, Hambleton, Talens, Debeaufort, Chiralt & Voilley, 2009;
36 Jafari, Bernaerts, Dodi & Shavandi, 2020; Weiss, Salminen, Moll & Schmitt, 2019).

37 For ionic polysaccharide like kappa-carrageenan (κ -Car), the upper critical solution
38 temperature (UCST) or the temperature above which a clear solution is observed strongly
39 depends on the ionic strength and the type of counter ions (Heyda, Soll, Yuan & Dzubiella,
40 2014). The charges on the polysaccharides interact with the charges on the other components
41 of mixed systems, for example, polysaccharides and proteins by repulsion or attraction and
42 this determines the texture of the system's steady state (Ako, Durand & Nicolai, 2011; Huang,
43 Mao, Li & Yang, 2021). In addition to the electrostatic interactions, polar and non-polar
44 interactions are also determinant in the equilibrium of the systems (Derkach, Kuchina,
45 Kolotova & Voron'ko, 2020). It has been shown that polar and non-polar interactions between
46 the polysaccharides and proteins are significantly affected by for example the conformational
47 transition (such as the coil-helix transition) of both components including unfolding of
48 proteins (Derkach, Kuchina, Kolotova & Voron'ko, 2020; Voron'ko, Derkach, Vovk &
49 Tolstoy, 2017; Weiss, Salminen, Moll & Schmitt, 2019). Since proteins may unfold and

50 expose polar and non-polar functional groups, attraction or repulsion interactions can emerge
51 following or opposing the electrostatic forces. Phase separation (segregation or association)
52 takes place if the mixed state correspond to a greater free energy than two separates phases
53 (Ako, Durand & Nicolai, 2011; Mezzenga & Fischer, 2013).

54 Below the UCST, the polysaccharide solutions can turn to aggregate suspensions, fluid gels
55 and gels, likewise, the viscosity of the solution increases to infinity at the gel point (Garrec,
56 Guthrie & Norton, 2013; Rochas & Rinaudo, 1984). The rheological properties of the
57 polysaccharide phase are crucial for the blending process, given that they contribute to the
58 stability of the suspensions (emulsion) and the microstructure of the systems (Derkach,
59 Kuchina, Kolotova & Voron'ko, 2020; Weiss, Salminen, Moll & Schmitt, 2019). However,
60 aggregation and gelation processes may not be achieved on a time-scale of processing and
61 observation, if the interactions between polysaccharide and water are still favorable even
62 below the UCST (Elfaruk, Wen, Chi & Li, 2021; Meunier, Nicolai & Durand, 2000).
63 Therefore, understanding the viscosity kinetic of the polysaccharide solutions and the
64 underlying mechanisms are necessary to predict the long-term stability of many
65 polysaccharide-based aqueous systems. The numerous works on polymer suspensions have
66 shown that the interactions between the polymers and solvent, thereby, intra/interchain
67 interactions, are determinant in the suspension viscosity (Bongaerts, Reynaers, Zanetti &
68 Paoletti, 1999; Colby, 2010; Croguennoc, Meunier, Durand & Nicolai, 2000; Elmarhoum &
69 Ako, 2022a).

70 The coil and helix states of carrageenan namely ι -Car, κ -Car and similar polysaccharide like
71 agarose has been extensively investigated by many authors in various aqueous and thermal
72 conditions using the optical rotation measurements or circular dichroism (Fujii, Yano,
73 Kumagai & Miyawaki, 2000; Gilsenan, Richardson & Morris, 2000; Mangione, Giacomazza,
74 Bulone, Martorana & San Biagio, 2003). At temperature below and equal the UCST, the

75 helices start to aggregate as soon as they are formed (Meunier, Nicolai & Durand, 2000;
76 Norton & Goodall, 1983). The correlation of the coil-helix transition with the abrupt change
77 of the suspension viscosity and visco-elasticity is well known from the numerous work
78 reported in the literature (Elmarhoum, Mathieu, Ako & Helbert, 2023; Meunier, Nicolai &
79 Durand, 2000; Rochas & Rinaudo, 1984). We took an advantage of existing research findings
80 to investigate the conformational change and aggregation kinetic of polysaccharides using
81 rheological methods. In a mixture of κ -Car and denatured β -lactoglobulin, the formation of
82 helices and aggregation of κ -Car were found to cause spherical domains of denatured β -
83 lactoglobulin similar to an emulsion (Ako, Durand & Nicolai, 2011). We hypothesize that the
84 control of the degree of helicity through the polysaccharide and water interactions could lead
85 to a better control of the structure of polysaccharide and protein mixtures. On one hand, a
86 lower helicity degree may cause lower aggregation/gelation rate (Meunier, Nicolai & Durand,
87 2000). On the other hand, a decrease of the polysaccharide and water attractive interactions is
88 expected to take place with an increase of the helicity degree (Tanaka & Wada, 1973).

89

90 **2 Materials and methods**

91 *2.1 The Polysaccharides*

92 The carrageenan polysaccharide is made of a repetition of disaccharide unit called carrabiose.
93 The carrabiose units, that form the neutral backbone of α -Car and κ -Car are composed of 3-
94 linked β -D-galactose (G) and 4-linked 3,6-anhydro-D-galactose (DA). For the two selected
95 carrageenans, only the position of the unique sulfate (S) group on the carrabiose is different
96 between them (Elmarhoum, Mathieu, Ako & Helbert, 2023). It is worth noting that the α -Car
97 as native polysaccharide does not exist naturally, but is made by a desulfation enzymatic
98 reaction from iota-carrageenan (ι -Car) coded as G4S-DA2S (Prechoux, Genicot, Rogniaux &

99 Helbert, 2013). Therefore, the κ -Car and α -Car are represented as G4S-DA and G-DA2S
100 respectively. The production of α -Car is a breakthrough in the study of carrageenan functional
101 properties, because they provide chemical or molecular origin information on the physical
102 properties of the widely studied κ -Car and ι -Car systems, namely the interaction between
103 these polysaccharides and water.

104 The κ -Car was a gift from RhodiaFood Switzerland (product name and reference: MEYPRO-
105 GEL 01/2001 WG95-37 K-Car) of an average molecular weight of 3.3×10^5 g/mol and
106 polydispersity index of $M_w/M_n = 2.0$, where M_w and M_n are the weight and number average
107 molar mass respectively.

108 The α -Car was a gift from Cermav (Centre de recherche sur les macromolécules végétales) of
109 average molecular weight of 3.8×10^5 g/mol and polydispersity index of $M_w/M_n = 1.8$.

110 2.2 *Preparation of the Samples*

111 The solutions of the two polysaccharides were prepared following the same preparation as
112 reported in our previous work (Elmarhoum, Mathieu, Ako & Helbert, 2023). The stock
113 solutions of the polysaccharide are dialyzed and free of added salts. The samples were
114 prepared by dilution to different concentrations of polysaccharide and salt (KCl) where
115 applicable. The samples with 0 mM salt indicate dilution of the stock solution with
116 demineralized water or as the polysaccharide solution in dialyzed form. The solutions with
117 salt were heated between 70 and 90 °C until they became completely transparent, ≈ 15 min,
118 then they were cooled prior to any use. These samples are considered as fresh samples only
119 during cooling and are no longer fresh if the cooling process was stopped. The cooling ramp
120 was 2 °C/min. The conservation of the sample before the measurements could last from 10 s
121 to 10 weeks. The aged samples were reset by heating before new measurements were
122 performed.

123

124 2.3 *Rheological measurements*

125 The viscosity of hydrocolloidal suspensions changes with the hydrocolloid's structural
126 properties. Therefore, the viscosity quantity is consistent for characterizing the aggregation of
127 hydrogel-forming polysaccharide in aqueous phase. Kinetics of the viscosity at different shear
128 rate and shear rate sweep of fresh and aged samples were performed in Couette geometry
129 using a DHR3 Rheometer (TA Instrument) with a thermo regulator (Microcool LAUDA
130 MC600) to control the temperature of the samples. The Couette geometry consisted of a
131 concentric cylinder geometry of an inner rotor cylinder (bob) and an outer stator cylinder
132 (cup) with radii R_1 of 14 mm and R_2 of 15 mm, respectively, defining a horizontal gap ($R_2 -$
133 R_1) of 1 mm and an average radius R of 14.5 mm as $(R_1 + R_2)/2$. The height of the bob was 42
134 mm, and the vertical gap between the bob and cup was set at 2 mm. The measurements were
135 done using similar experimental conditions as previously reported (Elmarhoum & Ako, 2021).

136 2.4 *Determination of critical concentration and statistical conditions*

137 The amount of solution of each concentration was prepared sufficiently to make at least three
138 samples. The measurements of the viscosity were performed on loaded sample with the same
139 run program more than twice after several cooling and heating, because the system is
140 thermoreversible. At least three samples of same polysaccharide / salt concentration were
141 analyzed at different days following the same protocol of mapping of the rheometer before the
142 samples were loaded onto the rheometer. In this experimental condition, the deviation of the
143 viscosity measurements is restricted to the size of the plot symbols except if indicated. The
144 viscosity (η_c) was plotted as function of polysaccharide concentrations for a given
145 temperature (T). The Kraemer specific viscosity was computed as $Ln(\eta_c / \eta_0)$, where η_0 is the
146 solvent viscosity, then this was divided by C and plotted as function of $Ln(C)$. The details on

147 this method have previously been reported (Ako, Elmarhoum & Munialo, 2022). We called
 148 this type of representation Kraemer-LogC (K-LogC) in relation with the Kraemer equation
 149 (Eq.1) commonly used to determine the Kraemer intrinsic viscosity $[\eta]_K$.

$$150 \quad \frac{\ln(\eta_c / \eta_0)}{C} = [\eta]_K + k \frac{[\eta]_K^2}{K} C \quad 1$$

151 Since the concentration dependence of the viscosity shows the dilute and semidilute regimes,
 152 the linear regression of the data in K-LogC representation of the two regimes cross at a
 153 concentration termed critical. The error bar or deviation applied to this critical concentration
 154 (C_c) is determined by an acceptable coefficient of determination which was here R^2 between
 155 0.85 and 1. Therefore, all the C_c values displayed in this work were obtained with $R^2 \geq 0.85$.

156 2.5 *Temperature dependence of the viscosity model*

157 The model is based on lower-viscosity-temperature (LVT) concept used to characterize the
 158 thermal property of the polysaccharide solutions.

$$159 \quad \eta^T = \eta^{T_{ref}} \cdot \exp[B_2 \cdot (T - T_{ref})(T - T_2)] \quad 2$$

160 where

$$161 \quad T_2 = 2T_c - T_{ref} \quad 3$$

162 and B_2 with T_c are adjusting parameters in respect of Ako et al., (2022) definition of these
 163 parameters (Ako, Elmarhoum & Munialo, 2022; Elmarhoum & Ako, 2022b). The quantity
 164 $B_2 \times T_c$ ($^{\circ}\text{C}^{-1}$) is less dependent on the adjustment, it was defined as the thermal expansion
 165 coefficient of the polymer chains. The T_c gives information on the free energy cost to break
 166 the interactions between polymer chains, therefore T_c is a bulk dependent phenomenon.
 167 However, to some extent we can hypothesize that monomer-monomer interchain interactions

168 could work for monomer-monomer intrachain interactions. For pure liquid, T_c characterizes
169 the temperature where molecular interactions become ineffective. But for small molecular
170 weight liquid like water, T_c could characterize the boiling point.

171

172 **3 Results and discussion**

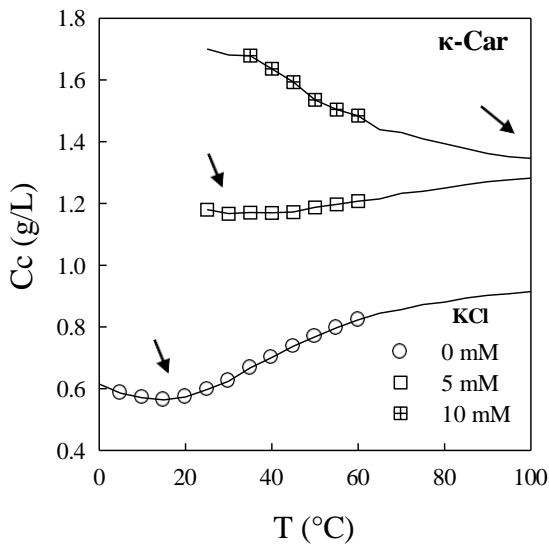
173 *3.1 The κ -Car and α -Car polysaccharide solutions*

174 Viscous flow is a kinetic phenomenon, whereas conformational characteristic is a result of
175 thermodynamic properties of the polymers in solution (Colby, 2010). Therefore, the
176 correlation between viscosity and conformational characteristic of the polysaccharide herein
177 is derived from Newtonian's flow of the polysaccharide solutions. The relationship between
178 the temperature and viscosity of κ -Car and α -Car solution characterizes the inter/intra
179 molecular interactions at work in the solution. Polysaccharide concentration dependence of
180 the relationship between the temperature and viscosity shed light on the thermodynamic
181 properties of κ -Car solution in the random coil state domain. Taking the dialyzed solution as
182 reference (0 mM), we have shown that if the KCl salt concentration (5 and 10 mM) is
183 increased, the temperature of characteristic critical concentration C_c (g/L) increases (Fig.1).
184 Common consideration of C_c (g/L) in polymer physical chemistry supposes that bulk and
185 excluded volume concentration should be the same at C_c (g/L). Therefore, considering that
186 excluded volume (V_p) is spherical, i.e., $V_p = 4\pi R_p^3/3$, at C_c (g/L) the concentration equal
187 m_p/V_p with m_p being the average mass of a single polymer in the V_p . With the polysaccharide
188 molecular mass M_p known, the expression of C_c (g/L) is given as:

189
$$C_c = \frac{3M_p}{4\pi R_p^3 N_A}$$

4

190 where the inverse of Avogadro's number, $1/N_A$, is the mol quantity of a single polymer. Given
 191 that the polysaccharide average mass is constant, the variation of C_c (g/L) as shown in Fig.1
 192 represents the polysaccharide volume in aqueous phase. The arrows in Fig.1 indicate the
 193 position of the minimum C_c (g/L) as well as the corresponding temperature named lower
 194 critical concentration temperature (LCCT).



195
 196 *Figure 1: Temperature dependence of critical concentration of the κ -Car solution for*
 197 *different KCl salt concentrations. The arrows indicate the lower C_c with its temperature. The*
 198 *C_c was determined with $R^2 \geq 0.85$. The solid lines are the results from the temperature-*
 199 *viscosity function (Eq.2).*

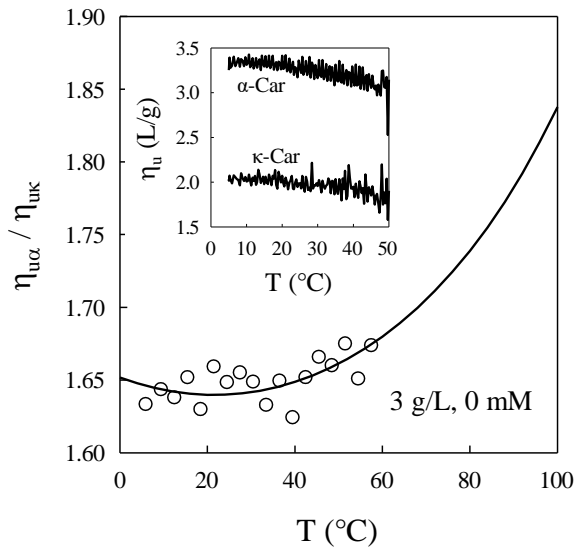
200 The minimum C_c (g/L) increases with the LCCT when the KCl salt concentration is
 201 increased. KCl salt concentration above 5 mM seems not applicable for determining the
 202 LCCT of κ -Car, therefore the results of 10 mM and above are simply indicative of the LCCT
 203 tendency. The particularly weak value of the KCl concentration stems from the ionic

204 selectivity property of κ -Car, which is characterized by a strong reaction in the presence of
205 KCl salt more than NaCl salt. The consequence of this selectivity is that gels of κ -Car exhibit
206 severe syneresis phenomenon in the presence of KCl rather than other food grade monovalent
207 salts. The thermodynamic origin of this phenomenon could be explained by the contraction of
208 the polysaccharide excluded volume, and accordingly, an increase of the solution C_c (g/L).
209 The polysaccharide excluded volume is the pervaded volume of chemically linear links and
210 physically cross links between the monosaccharide's molecules, and thus, is similar to a
211 physical and chemical nanohydrogel (nHG) particles. Considering the bulk as a compact
212 collection of such particles, viscosity, therefore, becomes a bulk flow issue of condensed
213 suspension of nHGs near the C_c (g/L). Correlation of the rheological properties of this
214 independently estimated volume is not illusory. Small and big nHG will lead to high and
215 weak C_c (g/L) respectively. Therefore, shrinking and swelling properties of the nHG are
216 derived from bulk flow in the polysaccharide concentration ranging below the entangled
217 concentration regime (Colby, 2010). In dilute solution regime, these properties are derived
218 from the polysaccharide intrachain interactions namely, hydrodynamic, excluded volume
219 effect, water-monosaccharide and carrabiose-carrabiose interactions. These intrachain
220 interactions determine the polysaccharide expansion and its conformational characteristics,
221 which is strongly dependent on the polysaccharide affinity for the liquid media in terms of
222 poor-, theta- and good-solvent. For the dialyzed solution, the κ -Car concentration dependence
223 of the viscosity was shown to increase following a scaling law, with a scaling power equal to
224 1.15. According to the scaling law theory of viscosity, a full repulsion between the carrabiose
225 should lead to a scaling power of 0.5 where neutral polymer in a good solvent yields 1.3. This
226 result supposes that intrachain interactions between the carrabioses are not fully repulsive and
227 the aqueous media is not good enough to promote full stretching of the polysaccharide. The
228 length scale of the polysaccharide chain that resists stretching or swelling is considered as the

229 unperturbed size (R_0) of the polysaccharide (Colby, 2010). Thus, we think that water
230 molecules should be out of this size domain due to excluded volume effect, because the free
231 energy or elastic energy cost to swell the nHG on length scales smaller than R_0 is huge
232 compared with Boltzmann energy (kT) and greater than the entropic energy. Conversely,
233 monosaccharide-monosaccharide attractive interactions should sharply decrease on length
234 scales larger than R_0 giving way for water-monosaccharide interactions to take place.

235 When κ -Car is converted to α -Car by the transfer of the sulfate group from the C4 of D-
236 galactose to the C2 of 3,6-anhydro-D-galactose, we can see a significant increase of the
237 viscosity of the dialyzed solution (Elmarhoum & Ako, 2022b). The specific viscosity per unit
238 of concentration, noted η_u (in L/g), is the property of polymer that is derived from
239 conformational characteristic as a result of excluded volume and water-polymer interactions.
240 These interactions respectively determine the C_c (g/L) and intrinsic viscosity of the system as
241 the limit of η_u when the polymer concentration decreased to 0 g/L (Ako, Elmarhoum &
242 Munialo, 2022). Therefore, the ratio between η_u of α -Car and κ -Car represents better the
243 conformational contribution to the viscosity difference between the two polysaccharides. The
244 temperature dependence of η_u of α -Car and κ -Car are displayed in the insert of Fig.2 as $\eta_{u\alpha}$
245 and $\eta_{u\kappa}$ respectively for the concentration of 3 g/L in dialyzed solution (0 mM). The Fig.2
246 shows the temperature dependence of $\eta_{u\alpha} / \eta_{u\kappa}$. These experimental measurement data are
247 shown in open circles and are fitted using the temperature-viscosity function reported in our
248 previous work (Eq.2) (Ako, Elmarhoum & Munialo, 2022).

249



250

251 *Figure 2: Temperature dependence of the ratio between α -Car reduced viscosity and κ -Car*
 252 *reduced viscosity. The insert shows the reduced viscosity of the two polysaccharides and the*
 253 *solid line is derived from the temperature-viscosity model (Eq.2).*

254 Though the specific viscosity per concentration shows a decreasing tendency with increasing
 255 temperature for both α -Car and κ -Car polysaccharides, it can see from the fit function in Fig.2
 256 that both the swelling and water molecules binding properties of κ -Car are more impaired by
 257 heat. Considering $f = \eta_{u\alpha} / \eta_{u\kappa}$, the fluctuation of f between 5 °C and 60 °C led to f being taken
 258 as an average value with a standard deviation of 1.65 ± 0.05 . In presence of 10 mM KCl and
 259 in the T-range [5 °C, 60 °C], the average quotient f was 1.70 ± 0.05 , which supposes that 10
 260 mM KCl salt impairs the swelling and binding water molecules properties of κ -Car compared
 261 with α -Car. The thermal expansion of κ -Car and α -Car nHG fit together with the coefficient
 262 $B_2 \times T_c = 1.5 \times 10^{-2} / ^\circ\text{C}$. However, the T_c are different as their values depend on the bulk
 263 concentration. We found for the concentration of 3 g/L, 141 °C for α -Car and 153 °C for κ -
 264 Car. Actually, the interaction potential between the nHG partially overlaps and this increases
 265 in intensity and density with the increase of the concentration above the C_c (g/L) (Elmarhoum
 266 & Ako, 2021). The regime of the concentration 3 g/L is semidilute for both systems and the

267 difference between their T_c may explain a difference in term of intensity and density of
268 monomer-monomer interchain interactions including the interaction between water and the
269 polysaccharides. With T_c of α -Car below the T_c of κ -Car, it implies that monomer-monomer
270 attractive interactions are greater for κ -Car than for α -Car in dialyzed solution. When 10 mM
271 KCl was added to the dialyzed solution and the solution was heated above 30 °C to melt κ -
272 Car aggregates and unfold the helices, the temperature dependence of the viscosity fits well
273 with the expansion coefficient $B_2 \times T_c$ and T_c of $1.4 \times 10^{-2} / ^\circ\text{C}$ and 183 °C respectively. The α -
274 Car solution with 10 mM KCl fits well with $1.55 \times 10^{-2} / ^\circ\text{C}$ and 139 °C respectively and did
275 not exhibit any features similar to the helix-coil conformational transition above 5 °C. The
276 addition of salt to the solutions shed light on the polyelectrolyte effect on the thermal
277 expansion properties of the polysaccharide including the repulsion interaction between the
278 monomers in both inter and intrachain interactions. Water and polysaccharide interactions are
279 influenced by salt accordingly. The 10 mM KCl salt has decreased the thermal expansion
280 coefficient of κ -Car nHGs and increased the monomer-monomer attractive interaction due to
281 screening electrostatic repulsion effect. The α -Car nHGs seems to not be sensitive as much as
282 κ -Car nHGs to 10 mM KCl, but a weak increase of the thermal expansion coefficient was
283 observed for α -Car. In addition to these results, we report a quotient f of 1.7 at 45 °C between
284 the η_u of α -Car and κ -Car at 3 g/L, the quotient f was found to increase from 1.5 to 1.8, if the
285 polysaccharide concentration is increased from 1 g/L to 5 g/L. We confirm by these results
286 the relative lower ability of κ -Car to expand and swell in monovalent aqueous phase, which
287 we have attributed to the sulfate group position effect in the carrabiose. The ionic selectivity
288 feature of these results was reported previously (Elmarhoum & Ako, 2022b; Elmarhoum,
289 Mathieu, Ako & Helbert, 2023).

290

291

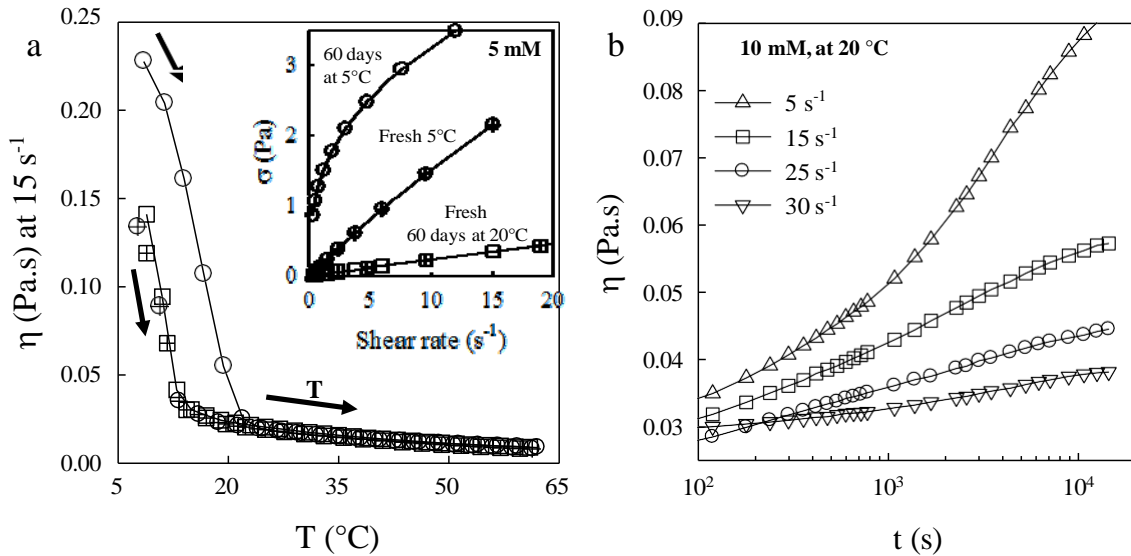
292 3.2 *The solution viscosity and self-assembly dynamic*

293 The formation of helices is reported for the conformational properties of hydrogel-forming
294 carrageenan (Bui, Nguyen, Renou & Nicolai, 2019; Ciancia, Milas & Rinaudo, 1997; Morris,
295 Rees & Robinson, 1980). The κ -Car polysaccharide in solution has shown prompt aggregation
296 and gelation properties particularly in the presence of KCl salt. The kinetics of both
297 mechanisms in competition influence the viscoelasticity of the samples. Therefore, when a
298 fresh solution of κ -Car in the presence of KCl is cooled to temperature range (T-range) below
299 the coil-helix temperature (T_{ch}), the viscosity of the fresh sample sharply increases, likewise,
300 the slope increases with the polysaccharide and salt concentrations (Meunier, Nicolai &
301 Durand, 2000; Meunier, Nicolai, Durand & Parker, 1999). Though aggregation promotes
302 gelation with increasing salt concentration at constant polysaccharide concentration, it could
303 be fatal for the gelation of the samples in the presence of a relatively high concentration of
304 KCl salt (100 mM) for weak polysaccharide concentrations (< 3 g/L).

305 Immediately, after cooling the fresh sample, if the sample was heated, the elasticity or
306 alternatively viscosity of the samples decreases to reach the viscosity of the solution above the
307 helix-coil temperature (T_{hc}) (Fig. 3a). The temperature hysteresis or gap between T_{ch} and T_{hc}
308 is reported as a result of the self-assembly property of the hydrocolloids. Therefore, the
309 viscosity stability of such hydrocolloid samples at a given temperature (T) depends not only
310 on their self-assembling kinetics (long-time viscosity property) but also on the real-time
311 property of the interactions between the hydrocolloids. Fresh and aged samples at $T > T_{hc}$, i.e.,
312 in random coil state, yield the same viscosity properties (insert of Fig. 3a). For example, the
313 sample with 5 mM are fresh at storage temperature of 20 °C even after 60 days (square
314 symbols in the insert of Fig. 3a), because their $T_{hc} = 15 \pm 2$ °C (square symbols in the Fig.
315 3a). Hence, no distinction was made between the samples conserved at temperature above T_{hc}
316 and the fresh or reset samples. However, the aged samples in T-range below T_{ch} have shown

317 distinctly two exciting viscosity properties: The real-time viscosity decreases with increasing
 318 the steady shear rate (open circles in the insert of Fig.3a) and the long-time viscosity increases
 319 with time at variable steady shear rate (Fig.3b).

320



321

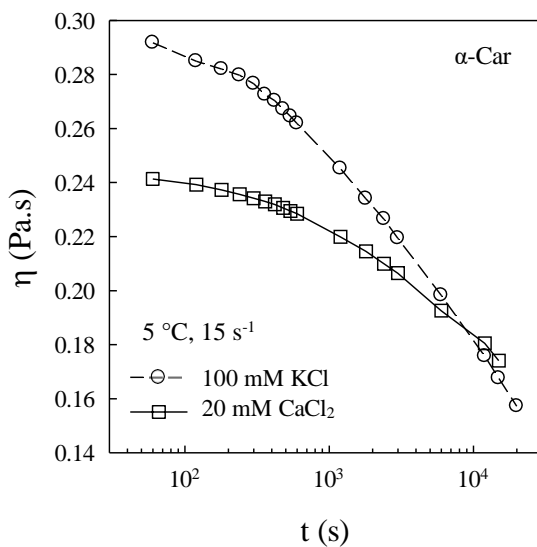
322 *Figure 3:a) Temperature dependence of the viscosity of κ -Car samples. The samples were*
 323 *loaded at 5 °C then heated to 60 °C. The open symbols are samples aged-at-rest for 60 days*
 324 *at 5 °C (circles) and at temperature above the helix-coil, 20 °C (squares). The crossed*
 325 *symbols are freshly prepared samples (circles) and reset to fresh from the aging samples*
 326 *(squares). The insert shows the shear rate dependence of the shear stress for the different*
 327 *tested samples. b) Kinetics of the viscosity of 3 g/L, κ -Car in presence of 10 mM KCl at 20 °C*
 328 *for different shear rates.*

329

330 The mechanisms underlying these observations stem from the polysaccharide-water and
 331 polysaccharide-polysaccharide interaction dynamics. The interaction dynamics and links
 332 between the helices part of the polysaccharide chains are determined by temperature and salt

333 concentrations. Some of them are broken and/or their formation impeded by the shear rate.
 334 We have surprisingly observed that unlike κ -Car, the viscosity of α -Car solution decreases
 335 with time under shear. We show the results in the Fig.4 for 3 g/L in the presence of 100 mM
 336 KCl and 20 mM CaCl_2 at 5 °C. Alpha-carrageenan shows less sensitivity to KCl salt as its
 337 solution in the presence of 100 mM KCl did not gel at time scale >12 h. Conversely, the
 338 CaCl_2 salt induces gelation of the polysaccharide and this was observed for 6 g/L but not for
 339 the duplicated 3 g/L samples at rest during the rheological tests. The coil-helix transitions of
 340 the polysaccharide were observed for 100 mM KCl and 20 mM CaCl_2 at ≈ 12 °C and 23 °C
 341 respectively. Comparatively, the gelation of α -Car is slower than the gelation of κ -Car and
 342 needs a considerable addition of a monovalent salt such as the gelation of the samples in
 343 presence of 400 mM KCl.

344



345

346 *Figure 4: Kinetics of the viscosity under shear rate 15 s⁻¹ of 3 g/L, α -Car in the presence of*
 347 *salt at 5 °C. Solid lines are guidelines for eyes*

348 The ionic sensitivity and viscosity property of both κ -Car and α -Car have evidenced the
349 chemical origin of their interactions with water. In actual sense, the two polysaccharides are
350 similar at a molecular level with one sulfate group being carried by their carrabiose, but the
351 position of the sulfate group is different. The transfer of the sulfate position from the C4 of D-
352 galactose (κ -Car) to the C2 of 3,6-anhydro-D-galactose (α -Car), turns the positive rate of the
353 viscosity kinetic (Fig. 3b) to negative (Fig. 4) with a significant impact on the ionic sensitivity
354 and selectivity. Hence, the carrageenan properties in aqueous phase are clearly determined by
355 the position of charges. Comparative analysis between the properties of κ -Car and α -Car with
356 other similar polysaccharides in aqueous phase has shown the role of the anhydro cycle,
357 charge, and the charge number carried by the polysaccharide monomers in their ionic
358 sensitivity, selectivity, and affinity with water (Elmarhoum & Ako, 2022a; Elmarhoum,
359 Mathieu, Ako & Helbert, 2023; Feke & Prins, 1974; Fujii, Yano, Kumagai & Miyawaki,
360 2000; Lindman, Karlström & Stigsson, 2010; Matsuo, Tanaka & Ma, 2002). For the selected
361 similar polysaccharide, there are neutral polysaccharides such as agarose which have an
362 anhydro cycle and cellulose without anhydro cycle. Agarose is a water-soluble polysaccharide
363 but cellulose is insoluble in water, though cellulose carries several -OH groups, and thus has a
364 good hydrogen bonding ability. We hypothesize that the anhydro cycle prevents a close
365 contact between the monomers carrying this functional group. Thus, the anhydro cycle
366 promotes the interaction between water and the monomers rather than interchain monomer
367 interactions. On one hand, we have the λ -Car without an anhydro cycle but its carrabiose
368 carries 3 anionic sulfate groups. The λ -Car does not gel in the presence of either mono or
369 divalent cations, it displays only viscous behavior (Running, Falshaw & Janaswamy, 2012).
370 Therefore, the charges prevent the contact between the monomers by electrostatic repulsion,
371 and thus promote water and monomers interactions better than the anhydro cycle. On the
372 other hand, we have the ι -Car with two anionic charges and anhydro cycle which is more

373 sensitive to divalent than monovalent counter ions, in the presence of which gelation of the ι -
374 Car solutions could happen (Bui, Nguyen, Renou & Nicolai, 2019; Elfaruk, Wen, Chi, Li &
375 Janaswamy, 2021). The κ -, ι - and λ -carrabiose with one, two and three anionic charges
376 respectively react selectively with mono, di and trivalent cations. Contrastingly α -carrabiose
377 carries one anionic charge but reacts preferentially with divalent cations rather than
378 monovalent cations. Finally, given that two or three monovalent cations do not work as one
379 divalent or trivalent respectively to reduce the intermolecular electrostatic repulsion, we
380 propose that salt valence should equal the carrabioses valence for a better electrostatic
381 reduction of their net charge(s). However, the anionic group on the 3,6-anhydro-D-galactose
382 is hindered by the anhydro cycle and this implies screening instead of binding ionic sites
383 mechanism (Ciancia, Milas & Rinaudo, 1997). Therefore, monovalent cations (K^+) are less
384 efficient to screen α -Car charge than divalent cation (Ca^{2+}). The screening of the mono
385 anionic charge on the α -Carrabiose by Ca^{2+} may turn the carrabiose net charge, $[carrabiose]^-$,
386 to partial positive charge, $[carrabiose, Ca^{2+}]^{+\delta}$ in accordance with obseravtion (Elmarhoum &
387 Ako, 2022a). However, the anionic group carried by κ -carrabiose is better exposed to the
388 binding with cations. When screening and/or binding sulfate ions promotes attractive
389 interactions between the monomers, intramolecular interactions take place preferentially.

390 The decrease of α -Car samples viscosities under 15 s^{-1} demonstrates that cross-links and
391 interhelical interaction dynamics respectively yield at applied steady shear stress and rate.
392 Furthermore, the initial viscosity of the tested α -Car samples are 10 times greater than the
393 viscosity of tested κ -Car samples with same polysaccharide concentration. Therefore, we
394 think that the α -Car helices self assembles into open aggregates which are less dense than
395 those formed in the κ -Car systems. As soon as the helices are nucleated, they form a bigger
396 size of swollen aggregate domains, thus they become more unstable under shear.

397 The shear rate (s^{-1}) defines the gradient of velocity between the inner rotor (bob) and outer
398 stator (cup) cylinder on gap of $\Delta R = 1$ mm. It interferes with the physical links properties in
399 the sample to determine the length scale δr , below which the sample remains thick and
400 unperturbed like a solid by the shearing. Under shear, the sample is arranged in layers number
401 N as $(\Delta R/\delta r)$. The thickness δr increases to bulk with decreasing shear rate toward $0 s^{-1}$, which
402 corresponds to the sample at rest. It is worth noting that, there is no real information on
403 viscosity below δr and that the samples viscosity should result from the interfaces (shear
404 band) between the stratum (δr). The cross-linking dynamics within the unperturbed layer
405 should lead to sizes of clusters no larger than δr . In this case, the time dependence of the
406 sample's viscosity at constant shear rate characterizes the dynamic and strength of
407 polysaccharide-polysaccharide interactions in balance with the interaction between
408 polysaccharide and water in the shear bands. If the links strength and frequencies of the cross-
409 linking and the helices stacking mechanisms are greater enough to overcome the shear stress
410 and rate, the viscosity of the sample should increase with time to stability when one of both
411 linking dynamic and strength fail against the shear rate or stress respectively. Actually, three
412 distinct points result from the viscosity properties of κ -Car show in Fig.3b.

413 In point (1) the viscosity increases with time because of connection kinetics between the
414 helices, indicating that the connections frequencies and strength are greater than the applied
415 shear rate and stress respectively.

416 In point (2) the viscosity stability is threshold by the shear rate and the decrease of the
417 viscosity with shear rate threshold indicates that the connections are characterized by multi-
418 frequencies cross-linking dynamic. Hence, all polysaccharide-polysaccharide linking
419 dynamics lower than the applied shear frequency no longer contribute to the gelation
420 mechanisms driven by the coil-helix conformational transition.

421 In point (3) the viscosity amplitude decreases if the shear rate, alternatively shear stress, is
422 increased. But, given that the samples were loaded in solution state prior to the links
423 formation, there is no information about the links strength in relation to the shear rate or
424 stress.

425 A strong liaison could be formed between the helices after several weeks and months in both
426 under shear and 0 shear conditions. We observed that the viscosities of aged-at-rest samples
427 decrease under increasing shear rate toward stability above the viscosity of fresh samples.
428 This observation is shown in the insert of Fig.3a for the 60 days aged sample at 5 °C as shear
429 rate dependence of the shear stress. Likewise, the links between helices are characterized by
430 multilevel of strength, therefore the shear stress acts like a shear stress threshold applicable on
431 mesoscopic scale (few number of stacking helices) (Meunier, Nicolai & Durand, 2000). For
432 this purpose, we define the stress threshold viscosity (η^S) and frequency threshold viscosity
433 (η^F) as the viscosity of aged-at-rest and fresh samples respectively when a steady shear stress
434 σ or rate $\dot{\gamma}$ is applied on the samples. The links in the aged-at-rest samples that may resist the
435 applied shear stress will remain in the unperturbed layer of thickness δr and the links that did
436 not sustain the applied shear stress will be progressively broken or disentangled in the shear
437 band to the yielded viscosity η^S . The stress threshold viscosity η^S and frequency threshold
438 viscosity η^F from aged-at-rest and fresh samples respectively are used to characterize the
439 gelation mechanisms driven by the helix-helix interactions. The thermodynamic properties of
440 these interchain connections strength determine the melting temperature, viscoelasticity of the
441 unperturbed layer's δr and viscosity properties of the aggregate suspensions and fluid gel.

442

443

444

445 3.3 Time dependence of viscosity of aggregating / gelling samples

446 Interchain interactions and further formation of connection between the polysaccharides may
447 lead to diverse sample characteristics. The solutions, aggregates suspensions, partially cross
448 linked aggregate suspensions (fluid gel), fine stranded or coarser gels are most of the sample's
449 characteristics reported in the literature (Bui, Nguyen, Renou & Nicolai, 2019; Garrec,
450 Guthrie & Norton, 2013; Hermansson, Eriksson & Jordansson, 1991; Rochas, Rinaudo &
451 Vincendon, 1980). However, these characteristics are determined by the kinetic and
452 thermodynamic properties of the polysaccharide conformational transition (coil-helix) and
453 interchain connections (Brunchi, Morariu & Bercea, 2014; Croguennoc, Meunier, Durand &
454 Nicolai, 2000). In the presence of KCl the kinetics of the coil-helix transition are very fast,
455 and nuclei are formed immediately at T_{ch} such that their contribution individually in the
456 sample's viscosity and kinetics are a complex issue. The viscosity kinetics are analyzed
457 through consideration of helices aggregation and/or percolation. Meunier et al., (2000) have
458 assumed two distinctly populations of the polysaccharides in solution for determining the
459 aggregation / gelation kinetics using light scattering measurements; one in fully helical
460 conformation and the other in coil conformation, though for the authors one may consider that
461 real polysaccharide would be partially in helical or coil state (Meunier, Nicolai & Durand,
462 2000; Tanaka & Wada, 1973). But the later coil state leads to non-aggregating samples
463 regarding the sample's viscosity properties and thus are stable. We have compared the η^F and
464 η^S at shear rate 5, 15 and 30 s^{-1} of different polysaccharide concentrations in the presence of 5,
465 10 and 15 mM KCl for 5 °C and 20 °C corresponding to the storage temperature of the
466 samples. The behaviors of the viscosity data are the same between the two-storage
467 temperatures. Moreover, not only does 5 °C work for the three KCl salt concentrations, but
468 also allows a better contrast between η^F and η^S . The results are shown in table 1 for the
469 storage samples at 5 °C. For these measurements, it is worth recalling that fresh samples are

470 reset from the aged ones and the η^F measurements were done in the same run after the η^S
 471 measurements by introducing in the measurement programs a heating and cooling temperature
 472 sweep of the initially aged samples. By doing this, we maintain the same concentrations as
 473 well as the instrument setting.

474 *Table 1: Viscosity at 5 ± 0.5 °C of κ -Car samples in various measurement conditions aged*
 475 *and fresh (reset) samples at 5, 15 and 30 s⁻¹ for 0.2 g/L to 9 g/L in presence of 5, 10, 15 mM*
 476 *KCl. A difference of ± 0.1 mPa.s between the viscosity values indicates significant difference*
 477 *between them in each row and column. After 60 days at 5 °C the solutions of 5 and 9 g/L in*
 478 *the presence of 10 and 15 mM KCl have gelled.*

| | | 0.2 g/L | 1 g/L | 5.0 g/L | 9.0 g/L | 0.2 g/L | 1.0 g/L | 0.2 g/L | 1.0 g/L |
|--------------------------|--------------------|-----------------------------------|----------|------------|------------|------------------------------------|------------|------------------------------------|------------|
| | | 5 mM KCl η (mPa.s) | | | | 10 mM KCl η (mPa.s) | | 15 mM KCl η (mPa.s) | |
| η^F , reset | 5 s ⁻¹ | 1.9 | 4.0 | 40.5 | 165.0 | 1.9 | 4.1 | 1.9 | 8.7 |
| η^S , 60 days after | | 2.0 | 4.5 | 127.7 | 522.4 | 2.7 | 22.7 | 3.6 | 59.2 |
| η^F , reset | 15 s ⁻¹ | 1.9 | 3.9 | 38.7 | 145.6 | 1.9 | 4.1 | 2.0 | 7.7 |
| η^S , 60 days after | | 1.9 | 4.4 | 84.7 | 253.3 | 2.5 | 14.7 | 3.1 | 28.8 |
| η^F , reset | 30 s ⁻¹ | 1.9 | 3.8 | 36.3 | 125.2 | 1.9 | 4.0 | 2.0 | 6.8 |
| η^S , 60 days after | | 1.9 | 4.3 | 63.6 | 166.6 | 2.4 | 11.2 | 2.8 | 19.4 |

479

480

481 The samples of 0.2 g/L in the presence of 5 mM at 5 °C were already stable above the shear
 482 rate of 5 s⁻¹ and interactions strength between the aggregates in suspension likely yield below
 483 a steady shear stress of 10 mPa. If the KCl concentration was increased to 10 mM, then to 15
 484 mM, the increment of viscosity between the fresh samples and aged-at-rest samples
 485 characterizes the interaction relaxation frequencies (shear rate in Hz) and the upper yield
 486 stress or link strength between aggregates in the suspension. In the presence of 10 mM and 15
 487 mM KCl, the interaction relaxation frequencies are likely a threshold < 5Hz for both salt
 488 concentration. However, when they are formed at rest (0 /s shear rate) in the presence of 10

489 mM and 15 mM KCl, some of the resulting links sustain applied steady shear stress of 73 mPa
490 and 85 mPa respectively. If now the concentration is increased to 1 g/L in the presence of 5
491 mM KCl, interaction frequencies above 30 Hz appear. Some of the links which are formed at
492 rest could resist shear stress above 129 mPa, however these links may not emerge under the
493 shear rate below 30 s^{-1} . The more the polysaccharide concentration and KCl salt, the faster the
494 formation of links. However, increasing KCl concentration to 15 mM did not accelerate the
495 links formation between nuclei for 0.2 g/L. We think that diffusion coefficient likely limited
496 the nuclei aggregation. Therefore, a critical concentration may exist between 0.2 g/L and 1
497 g/L at which, the nuclei cross linking dependence on diffusion phenomenon is negligible. This
498 concentration could be close to the critical concentration C_c (g/L) of the polysaccharide in
499 coil state and may characterize the concentration of true gel formation (Meunier, Nicolai &
500 Durand, 2000). For instance, the samples of 0.5 g/L, κ -Car did not form a true gel (simply by
501 tilting the container) after 60 days at 5°C in the presence of KCl concentration ranging below
502 50 mM, while the samples of 1 g/L gelled in the presence of 25 mM, KCl but collapsed to
503 liquid samples in the presence of 100 mM KCl.

504 The polysaccharide needs to overlap their potential of interactions in solutions at least
505 partially prior to finding the salt conditions for the sample gelation. In this case, the
506 polysaccharide conformational states are rather relevant than their random motions (Lin,
507 Lindsay, Weitz, Ball, Klein & Meakin, 1989; Savel'ev, Marchesoni, Taloni & Nori, 2006;
508 Tanaka & Wada, 1973). Hence, the viscosity kinetics would therefore result from
509 conformational transition evolution from fine stranded filaments to stiff segments. However,
510 interconnections speed and strength between the filaments and stacking domains of the stiff
511 segments could be weakened by decreasing either the salt, polysaccharide concentration or
512 both. For these types of systems, the concentration of solid matter is not sufficient to
513 determine the thermodynamic chemical potential. Because of its critical role, we may

514 consider or define the conformational transition as a potential of activity of the polysaccharide
515 in solution, which activity influence the viscosity. However, a number of questions emerge
516 such as (i) what is the optimum degree of the helix conformation in a given aqueous phase
517 which characterizes the thermodynamic stability of the polysaccharide system? and (ii) how
518 does the polysaccharide concentration regimes (dilute, semidilute, entangled) influence the
519 helix optimum degree? The optical rotation of κ -Car reaches with time different degrees in
520 function of combined ionic strength and temperature effects. Its rate is also influenced and
521 equilibrium was not clearly demonstrated by the system after 12 h in log time scale (Meunier,
522 Nicolai & Durand, 2000). It is well known from earlier reports on salt effects that KCl
523 particularly promotes stiffness and stacking domains for κ -Car in solution (Ako, 2015;
524 Hermansson, 1989; Hermansson, Eriksson & Jordansson, 1991). But these local phase
525 separation processes could be fatal to the sample water holding capacity and macroscopic
526 stability. Understanding their kinetics will contribute to resolving the origin of the resulting
527 instabilities.

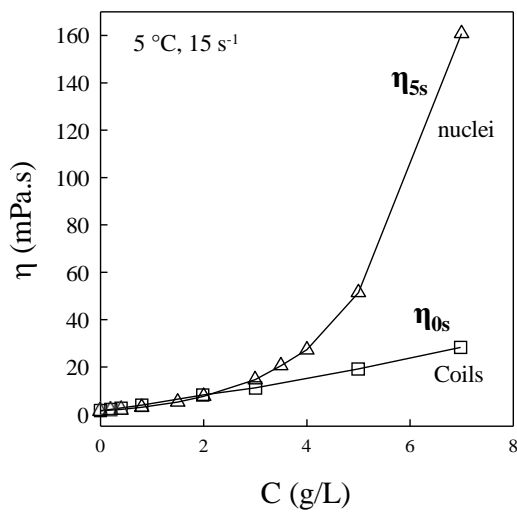
528

529 *3.4 Influence of concentration on sample's viscosity kinetic*

530 For all the samples exhibiting a coil-helix transition, kinetics of the sample's viscosity was
531 done at constant temperature below the coil-helix temperature (T_{ch}). The time delay to cool
532 the solution from T_{ch} to the kinetics measurement temperatures depends on the cooling rate.
533 For an example, the solutions in the presence of 10 mM KCl show a $T_{ch} = 25$ °C, hence it
534 takes 10 min to cool the solutions from 25 °C to 5 °C with a cooling rate of 2 °C/min during
535 which the nucleation and nuclei characteristics of the solutions change following the
536 temperature variation. The kinetics started immediately, which means 5 s for the first
537 viscosity value at the measurement temperature. Because instantaneously connected helices

538 occur in the sample as soon as the temperature has reached T_{ch} , the viscosity dependently may
 539 result from the presence of nuclei in the sample between 0 and 5 s (Fig.5). In terms of the
 540 sample viscosities, 0 and 5 s correspond to the viscosity of the samples without salt and the
 541 first viscosity value at the measurement temperature respectively. The cooling rate was 2
 542 $^{\circ}\text{C}/\text{min}$ and shear rate by default was 15 s^{-1} for all samples tested unless otherwise specified.

543



544

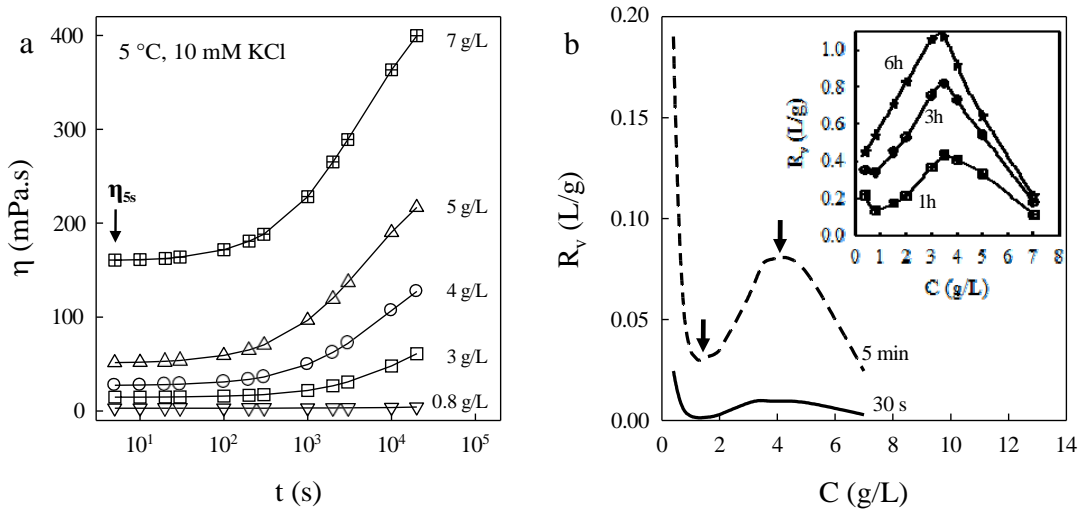
545 *Figure 5: Concentration dependence of viscosity of κ -Car solution in the presence of 0 and 10*
 546 *mM KCl salt at 5 $^{\circ}\text{C}$ under shear rate of 15 s^{-1} . The η_{5s} is the viscosity at 5 s after the*
 547 *temperature is set at 5 $^{\circ}\text{C}$ and η_{0s} is the viscosity without added salt. The solid lines are*
 548 *guidelines for eyes.*

549 The helices start to aggregate as soon as they are nucleated and because of time imprecision
 550 on the nucleation kinetic we may consider the measurements beginning time step ($\delta t = 5\text{ s}$),
 551 hence η_{5s} is considered as a threshold, and anything that may happen further in the sample is
 552 therefore due to only interactions and physical bounds formation between the nuclei
 553 prevailing in the samples within δt . Hence, the viscosity at any time t , η_t , minus η_{5s} is divided
 554 by η_{5s} and polysaccharide concentration to give the reduced relative increment viscosity, R_v

555 (L/g). The reduced viscosities R_v (L/g) are determined for all tested samples (Eq.5) as a
 556 function of time and concentration. Taking variable time window from the viscosity kinetics
 557 in Fig.6a, for examples 30 s, 5 min, 1 h, 3 h and 6h, the concentration dependence of R_v were
 558 determined (Fig.6b) to analyze the effects of interactions through the polysaccharide
 559 concentrations influence on the viscosity kinetics. Indirectly, the analysis may provide some
 560 relevant conclusions on the conformational dynamics dependence on polysaccharide
 561 concentration for a given condition of temperature, salt concentration and shear rate.

562
$$R_v = \frac{\eta_t - \eta_{ss}}{\eta_{ss} \cdot C}$$
 5

563



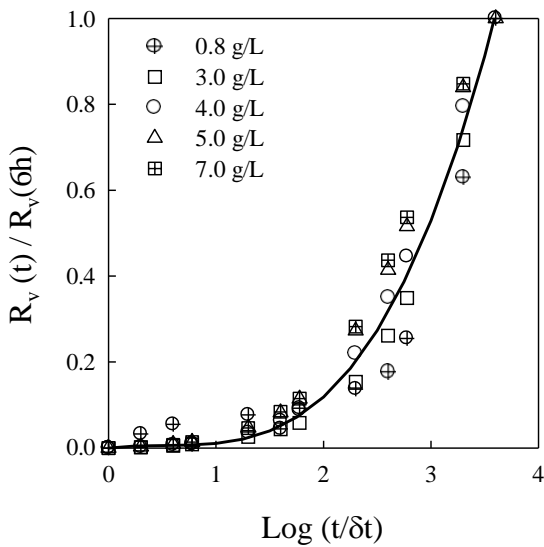
564

565 *Figure 1: a) Kinetics of the viscosity under 15 s^{-1} for different κ -Car concentrations in*
 566 *presence of 10 mM KCl. b) Concentration dependence of the relative increment viscosity per*
 567 *unit of concentration (R_v) for different selected time steps, 30 s, 5 min and 1h, 3h, 6h (insert).*
 568 *Solid lines are guidelines for eyes.*

569 The time dependence of viscosity of higher polysaccharide concentration evolves above lower
 570 polysaccharide concentration samples, because the viscosity of the samples at the beginning

571 η_{5s} increases with increasing polysaccharide concentration. The logarithmic scale of time
572 shows that the viscosity of the samples still increases and is not about to reach equilibrium.
573 However, the reduced viscosities in Fig.6b show an interesting behavior with concentration,
574 which is characterized by two characteristic concentrations in C-range between 0.2 g/L and 7
575 g/L. If we take the viscosity values of the samples in time step of 30 s, we observe that the
576 relative viscosity starts to increase and to decrease from roughly the concentration of 1 ± 0.5
577 g/L and 3.5 ± 0.5 g/L respectively. Time steps above 30 s show the same extreme of
578 concentration, but the increase and decrease of the reduced viscosity after 3 h are stiff within
579 the C-range from 1 g/L to 3.5 g/L and from 3.5 g/L to 7 g/L with respectively a slop of 0.23
580 and 0.24 (insert of Fig.6b). Given that the viscosity increase with time is observed for all the
581 samples, the decrease of reduced viscosity in C-range from 3.5 g/L to 7 g/L is not in
582 agreement with both concentration and viscosity increase (Garrec, Guthrie & Norton, 2013).
583 Therefore, although helix degree and number of interchain connections increase with time,
584 this is likely not to happen in agreement with the increase of polysaccharide concentration
585 above a characteristic maximum polysaccharide concentration (3.5 ± 0.5 g/L in this case). In
586 any given aqueous phase and above the critical concentration from which the conformational
587 transitions control the aggregation/gelation mechanisms rather than the polysaccharide
588 diffusion coefficient, the increase of polysaccharide concentration beyond the characteristic
589 maximum polysaccharide concentration will hinder or freeze the conformational kinetic to a
590 certain degree. The effect may either delay the interactions and connection degrees in time,
591 strengthen or result in both a delay and a strengthening. The delay in strength means the same
592 kinetics, but with weak reduced viscosity. The delay in time means the same reduced
593 viscosity will be found for higher concentration, but at a later time. Vertical and horizontal
594 shift of the reduced viscosities dependence on time could help to at least conclude on whether
595 lower and higher concentration follow the same kinetics and connection strength development

596 or not. To shift the reduced threshold viscosity, we simply divided the time dependence of the
 597 reduced threshold viscosities by their values at time step of 6h. The time axis is displayed in
 598 logarithmic scale of $t/\delta t$ with $\delta t = 5$ s. As we can see in Fig.7, all the samples of concentration
 599 above the characteristic minimum concentration of 1 ± 0.5 g/L, fall on the same master curve
 600 acceptably (see the guideline for eye in Fig.7). The result, we think is an indication that the
 601 samples of concentration above ≈ 1 g/L follow roughly same kinetics but with different links
 602 strength between the polysaccharide in either filaments, helices, or aggregate forms.



603
 604 *Figure 2: Master curve of the reduced viscosity kinetics for all the samples concentration*
 605 *displayed in Fig.6a. The $\delta t = 5$ s is the time for the measurement beginning and 6 h is the*
 606 *total time of the kinetics measurement. Solid line is a guideline for eyes.*

607
 608 The samples below 1 g/L, for instance 0.4 g/L and 0.2 g/L tested, are not on the master
 609 kinetics curve because their concentrations fall in dilute concentration regime, accordingly
 610 interchain liaisons are likely not dominant. Alternatively, the viscosity kinetic properties of
 611 these samples likely result from intrachain rather than interchain interactions and aggregations

612 are controlled by diffusion. However, coil-helix transition without aggregation (lower
613 concentration) seems to have lower impact on viscosity kinetics. Two months later, the
614 samples of concentration above 4 g/L in the presence of 10 mM had gelled at rest.
615 Considering this result with the fact that viscosity of the samples in C-range between ≈ 1 g/L
616 and 7 g/L (tested) follow roughly the same kinetics, we may hypothesize that after months
617 and years under 15 s^{-1} shear rate at $5\text{ }^{\circ}\text{C}$, the concentration dependence of reduced threshold
618 viscosity of the samples between ≈ 1 g/L and 3.5 g/L with ≈ 3.5 g/L and 7 g/L may finally fall
619 on the same negative slope. Hence, may be the samples ranging below 1 g/L could show an
620 increase of reduced threshold viscosity as a function of concentration. Accordingly, the
621 characteristic maximum concentration initially found at ≈ 3.5 g/L could after several hours,
622 days or months shift to ≈ 1 g/L and the characteristic minimum concentration initially at ≈ 1
623 g/L will be shifted to let's say the C_c (g/L) or may be lower after years. The study of the
624 polysaccharide in solution demonstrates that affinity between polysaccharide and water is
625 better when the polysaccharide is in coil than helix conformational state. Therefore, according
626 to our analysis, it results that the affinity of polysaccharide to water property is not a
627 colligative but a conformational issue. For κ -Car, the affinity would increase because helix
628 degree decreases with increasing the polysaccharide concentration in even potassium aqueous
629 phase.

630 **4 Conclusion**

631 Polysaccharide properties in aqueous phase strongly influence the process, texture, and
632 stability of polysaccharide-based mixtures. Given that conformational changes influence
633 directly the viscosity of many polysaccharides in aqueous mixtures, the degree of helicity that
634 controls kappa-carrageenan (κ -Car) interaction with water was derived from the viscosity
635 properties of κ -Car in aqueous phase. The coil and helix conformation of κ -Car correlates

636 with stable viscosity over a time scale of 60 days and with a continuous increase in the
637 viscosity over undetermined time scale. So far, this evolution of the viscosity is attributed to
638 the aggregation of the helices toward the system gelation considering that the helicity degree
639 of the polysaccharide is stabilized. We conclude from this current study that the κ -Car helicity
640 is stabilized by increasing the polysaccharide concentration at a degree more and more lower
641 than the thermodynamic degree of the polysaccharide helicity, which is determined by the
642 ionic strength, type of counter ions, and temperature. Therefore, the concentration regime of
643 the suspensions is crucial for determining the κ -Car helicity degree from which the
644 interactions with water and other type of components in the systems as well as aggregation
645 and gelation occur. Comparing the properties of κ -Car with α -Car and other similar
646 polysaccharides, we have emphasized the role of the chemical structure on their interactions
647 with water, e.g., the anhydro function of the saccharide moieties with sulfate groups promotes
648 better polysaccharide-water interactions than the saccharide moieties with only sulfate groups
649 and much more better than neutral saccharide moieties.

650 **Acknowledgements**

651 We thank Professor William Helbert from the Centre de Recherche sur les Macromolécules
652 Végétales (CERMAV) for the α -Carrageenan and Vincent VERDOOT for his technical
653 assistance with the rheometer instruments. This work was financially supported by I-MEP2
654 PhD graduate school and the PolyNat Carnot Institut. The Laboratoire Rhéologie et Procédés
655 (LRP) is part of LabEx Tec 21 (Investissements d'Avenir - grant agreement n°ANR-11-
656 LABX-0030) and PolyNat Carnot Institut (Investissements d'Avenir - grant agreement
657 n°ANR-11-CARN-030-01).

658 **Declaration of competing interest**

659

660 **The authors declare no conflicts of interest.**

661 **References**

662

663 Ako, K. (2015). Influence of elasticity on the syneresis properties of kappa-carrageenan gels.

664 *Carbohydrate Polymers*, 115, 408-414.

665 Ako, K., Durand, D., & Nicolai, T. (2011). Phase separation driven by aggregation can be

666 reversed by elasticity in gelling mixtures of polysaccharides and proteins. *Soft Matter*, 7,

667 2507-2516.

668 Ako, K., Elmarhoum, S., & Munialo, C. D. (2022). The determination of the lower critical

669 concentration temperature and intrinsic viscosity: The syneresis reaction of polymeric gels.

670 *Food Hydrocolloids*, 124, 107346.

671 Bongaerts, K., Reynaers, H., Zanetti, F., & Paoletti, S. (1999). Equilibrium and

672 nonequilibrium association processes of κ -carrageenan in aqueous salt solutions.

673 *Macromolecules*, 32, 683-689.

674 Brunchi, C.-E., Morariu, S., & Bercea, M. (2014). Intrinsic viscosity and conformational

675 parameters of xanthan in aqueous solutions: Salt addition effect. *Colloids and Surfaces B*, 122,

676 512-519.

677 Bui, V. T. N. T., Nguyen, B. T., Renou, F., & Nicolai, T. (2019). Rheology and

678 microstructure of mixtures of iota and kappa-carrageenan. *Food Hydrocolloids*, 89, 180-187.

679 Ciancia, M., Milas, M., & Rinaudo, M. (1997). On the specific role of coions and counterions

680 on kappa-carrageenan conformation. *International Journal of Biological Macromolecules*, 20,

681 35-41.

682 Colby, R. H. (2010). Structure and linear viscoelasticity of flexible polymer solutions:

683 comparison of polyelectrolyte and neutral polymer solutions. *Rheologica Acta*, 49, 425-442.

684 Croguennoc, P., Meunier, V., Durand, D., & Nicolai, T. (2000). Characterization of

685 semidilute κ -carrageenan solutions. *Macromolecules*, 33, 7471-7474.

686 Derkach, S. R., Kuchina, Y. A., Kolotova, D. S., & Voron'ko, N. G. (2020). Polyelectrolyte
687 polysaccharide-gelatin complexes: Rheology and structure. *Polymers*, *12*, 266.

688 Einhorn-Stoll, U. (2018). Pectin-water interactions in foods - From powder to gel. *Food*
689 *Hydrocolloids*, *78*, 109-119.

690 Elfaruk, M. S., Wen, C., Chi, C., & Li, X. (2021). Effect of salt addition on iota-carrageenan
691 solution properties. *Food Hydrocolloids*, *113*, 106491.

692 Elfaruk, M. S., Wen, C., Chi, C., Li, X., & Janaswamy, S. (2021). Effect of salt addition on
693 iota-carrageenan solution properties. *Food Hydrocolloids*, *113*, 106491.

694 Elmarhoum, S., & Ako, K. (2021). Lower critical concentration temperature as
695 thermodynamic origin of syneresis: Case of kappa-carrageenan solution. *Carbohydrate*
696 *Polymers*, *267*, 118191.

697 Elmarhoum, S., & Ako, K. (2022a). Rheological study of alpha- and kappa-carrageenan
698 expansion in solution as effects of the position of the sulfate group. *International Journal of*
699 *Biological Macromolecules*, *223*, 1138-1144.

700 Elmarhoum, S., & Ako, K. (2022b). Rheological study of α - and κ -carrageenan expansion in
701 solution as effects of the position of the sulfate group. *International Journal of Biological*
702 *Macromolecules*, *223*, 1138-1144.

703 Elmarhoum, S., Mathieu, S., Ako, K., & Helbert, W. (2023). Sulfate groups position
704 determines the ionic selectivity and syneresis properties of carrageenan systems.
705 *Carbohydrate Polymers*, *299*, 120166.

706 Fabra, M. J., Hambleton, A., Talens, P., Debeaufort, F., Chiralt, A., & Voilley, A. (2009).
707 Influence of interactions on water and aroma permeabilities of iota-carrageenan-oleic acid-
708 beeswax films used for flavour encapsulation. *Carbohydrate Polymers*, *76*, 325-332.

709 Feke, G. T., & Prins, W. (1974). Spinodal phase separation in a macromolecular sol-gel
710 transition. *Macromolecules*, *7*, 527-530.

711 Felfel, R. M., Gideon-Adeniyi, M. J., Hossain, K. M. Z., Roberts, G. A. F., & Grant, D. M.
712 (2019). Structural, mechanical and swelling characteristics of 3D scaffolds from chitosan-
713 agarose blends. *Carbohydrate Polymers*, *204*, 59-67.

714 Fujii, T., Yano, T., Kumagai, H., & Miyawaki, O. (2000). Scaling analysis on elasticity of
715 agarose gel near the sol-gel transition temperature. *Food Hydrocolloids*, *14*, 359-363.

716 Garrec, D. A., Guthrie, B., & Norton, I. T. (2013). Kappa carrageenan fluid gel material
717 properties. Part 1: Rheology. *Food Hydrocolloids*, *33*, 151-159.

718 Gerentes, P., Vachoud, L., Doury, J., & Domard, A. (2002). Study of a chitin-based gel as
719 injectable material in periodontal surgery. *Biomaterials*, *23*, 1295-1302.

720 Gilsenan, P. M., Richardson, R. K., & Morris, E. R. (2000). Thermally reversible acid-
721 induced gelation of low-methoxy pectin. *Carbohydrate Polymers*, *41*, 339-349.

722 Hermansson, A.-M. (1989). Rheological and microstructural evidence for transient states
723 during gelation of kappa-carrageenan in the presence of potassium. *Carbohydrate Polymers*,
724 *10*, 163-181.

725 Hermansson, A.-M., Eriksson, E., & Jordansson, E. (1991). Effects of potassium, sodium and
726 calcium on the microstructure and rheological behaviour of kappa-carrageenan gels.
727 *Carbohydrate Polymers*, *16*, 297-320.

728 Heyda, J., Soll, S., Yuan, J., & Dzubiella, J. (2014). Thermodynamic description of the LCST
729 of charged thermoresponsive copolymers. *Macromolecules*, *47*, 2096-2102.

730 Huang, M., Mao, Y., Li, H., & Yang, H. (2021). Kappa-carrageenan enhances the gelation
731 and structural changes of egg yolk via electrostatic interactions with yolk protein. *Food*
732 *Chemistry*, *360*, 129972.

733 Jafari, H., Bernaerts, K. V., Dodi, G., & Shavandi, A. (2020). Chitooligosaccharides for
734 wound healing biomaterials engineering. *Materials Science and Engineering C*, *117*, 111266.

735 Lin, M. Y., Lindsay, H. M., Weitz, D. A., Ball, R. C., Klein, R., & Meakin, P. (1989).
736 Universality in colloid aggregation. *Nature*, *339*, 360-362.

737 Lindman, B., Karlström, G., & Stigsson, L. (2010). On the mechanism of dissolution of
738 cellulose. *Journal of Molecular Liquids*, *156*, 76-81.

739 Mangione, M. R., Giacomazza, D., Bulone, D., Martorana, V., & San Biagio, P. L. (2003).
740 Thermoreversible gelation of kappa-carrageenan: relation between conformational transition
741 and aggregation. *Biophysical Chemistry*, *104*, 95-105.

742 Matsuo, M., Tanaka, T., & Ma, L. (2002). Gelation mechanism of agarose and κ -carrageenan
743 solutions estimated in terms of concentration fluctuation. *Polymer*, *43*, 5299-5309.

744 Meunier, V., Nicolai, T., & Durand, D. (2000). Structure and kinetics of aggregating kappa-
745 carrageenan studied by light scattering. *Macromolecules*, *33*, 2497-2504.

746 Meunier, V., Nicolai, T., Durand, D., & Parker, A. (1999). light scattering and viscoelasticity
747 of aggregating and gelling kappa-carrageenan. *Macromolecules*, *32*, 2610-2616.

748 Mezzenga, R., & Fischer, P. (2013). The self-assembly, aggregation and phase transitions of
749 food protein systems in one, two and three dimensions. *Reports on Progress in Physics*, *76*,
750 046601-046643.

751 Morris, E. R., Rees, D. A., & Robinson, G. (1980). Cation-specific aggregation of
752 carrageenan helices : Domain model of polymer gel structure. *Journal of Molecular Biology*,
753 *138*, 349-362.

754 Norton, I. T., & Goodall, D. M. (1983). Equilibrium and dynamic studies of the disorder-
755 order transition of kappa-carrageenan. *J. Chem. Soc., Faraday Trans. 1*, *79*, 2489-2500.

756 Prechoux, A., Genicot, S., Rogniaux, H., & Helbert, W. (2013). Controlling carrageenan
757 structure using a novel formylglycine-dependent sulfatase, an Endo-4S-iota-carrageenan
758 sulfatase. *Marine Biotechnology*, *15*, 265-274.

759 Rochas, C., & Rinaudo, M. (1984). Mechanism of gel formation in κ -Carrageenan.
760 *Biopolymers*, 23(4), 735-745.

761 Rochas, C., Rinaudo, M., & Vincendon, M. (1980). Structural and conformational
762 investigation of carrageenans. *Biopolymers*, 19(12), 2165-2175.

763 Running, C. A., Falshaw, R., & Janaswamy, S. (2012). Trivalent iron induced gelation in
764 lambda-carrageenan. *Carbohydrate Polymers*, 87, 2735-2739.

765 Saeedi Garakani, S., Khanmohammadi, M., Atoufi, Z., Kamrava, S. K., Setayeshmehr, M.,
766 Alizadeh, R., Faghihi, F., Bagher, Z., Davachi, S. M., & Abbaspourrad, A. (2020). Fabrication
767 of chitosan/agarose scaffolds containing extracellular matrix for tissue engineering
768 applications. *International Journal of Biological Macromolecules*, 143, 533-545.

769 Savel'ev, S., Marchesoni, F., Taloni, A., & Nori, F. (2006). Diffusion of interacting Brownian
770 particles: Jamming and anomalous diffusion. *Physical Review E*, 74, 1-9 (021119).

771 Tanaka, T., & Wada, A. (1973). Dynamical aspects of helix-coil transitions in biopolymers.
772 *J. Chem. Phys.*, 59, 3799-3810.

773 Voron'ko, N. G., Derkach, S. R., Vovk, M. A., & Tolstoy, P. M. (2017). Complexation of
774 kappa-carrageenan with gelatin in the aqueous phase analysed by ^1H NMR kinetics and
775 relaxation. *Carbohydrate Polymers*, 169, 117-126.

776 Weiss, J., Salminen, H., Moll, P., & Schmitt, C. (2019). Use of molecular interactions and
777 mesoscopic scale transitions to modulate protein-polysaccharide structures. *Advances in*
778 *Colloid and Interface Science*, 271, 101987.

779 Yousefi, A. R., & Ako, K. (2020). Controlling the rheological properties of wheat starch gels
780 using lepidium perfoliatum seed gum in steady and dynamic shear. *International Journal of*
781 *Biological Macromolecules*, 143, 928-936.

782

783